Multi-Dimensional Systems Built from Dichromate Anions − Syntheses, Crystal Structures, and Magnetic Properties

Xiao-Yan Chen,[a] Bin Zhao,[a] Peng Cheng,*[a] Bin Ding,[a] Dai-Zheng Liao,[a] Shi-Pin Yan,[a] and Zong-Hui Jiang[a]

Keywords: Chromium / Magnetic properties / N ligands / Self-assembly

Three novel compounds with bridging dichromate anions with the formulae $[Fe(4,4'\text{-bpy})_2Cr_2O_7]_n$ (**1**), $[Co(4,4'\text{-bpy})_2Cr_2O_7]_n$ (**2**), and $[Ni(dpa)_2Cr_2O_7]\cdot H_2O$ (**3**) (4,4′-bpy = 4,4′-bipyridine, dpa = 2,2′-dipyridylamine) have been synthesized and characterized. The isostructural compounds **1** and **2** belong to the monoclinic space group *C*2/*c* and have been shown to be three-dimensional polymers in which the dichromate anions connect neighboring layers formed by $[M(4,4'\text{-bpy})_2]^{2+}$ (M = Fe, Co) units. Compound **3** is a metallacrown type compound, crystallizing in the monoclinic space group $P2_1/n$. Two chromate anions link two Ni^{II} centers forming a dinuclear entity. The uncoordinated oxygen atom of the dichromate anion forms a hydrogen bond with the N–H unit of dpa resulting in a two-dimensional network. Measurements of magnetic susceptibilities indicate the presence of antiferromagnetic interactions in **1** and **2** whereas the exchange coupling between the Ni^{II} ions in **3** is ferromagnetic. The IR and UV/Vis spectra of the above complexes have also been investigated.

(© Wiley-VCH Verlag GmbH & Co. KGaA, 69451 Weinheim, Germany, 2004)

Introduction

Investigations of novel inorganic-organic hybrid framework assemblies constitute one of the most active areas of material science and chemical research. The intense interest in these materials has been driven, to a large extent, by their interesting properties such as electrical conductivity, magnetism, photo-mechanistic behavior, and shape specificity as well as their potential applications in areas such as catalysis.[1−3] Many important properties of supramolecular systems depend largely on their structures and topologies. Rational design and construction of new materials with specific networks has therefore become a particularly important and topical subject.[4,5]

The chromate ion has long been known to bridge metal centers forming oligomeric and polymeric systems and many chromate bridged polynuclear complexes have been characterized.[6−9] On the other hand we know that between the physiologically accessible pH values of 2−6 the $HCrO_4^-$ and $Cr_2O_7^{2-}$ ions are in equilibrium.[10] Whereas many structural studies of simple or double "inorganic" dichromates have been reported,[11] the use of the dichromate anion as a bridging ligand forming multi-dimensional networks needs to be explored more deeply.[12,13]

We started to design hybrid complexes with dichromate anions and the typical polypyridine system which is well-known to act as a rigid, rod-like organic building block. In this paper we report the synthesis and structural characterization of three dichromate polymers, $[Fe(4,4'\text{-bipy})_2Cr_2O_7]_n$ (**1**), $[Co(4,4'\text{-bipy})_2Cr_2O_7]_n$ (**2**), and $[Ni(dpa)_2Cr_2O_7]\cdot H_2O$ (**3**) (4,4′-bpy = 4,4′-bipyridine, dpa = 2,2′-dipyridylamine). Furthermore, their magnetic and spectroscopic properties have also been studied.

Results and Discussion

Crystal Structure of $[Fe(4,4'\text{-bpy})_2Cr_2O_7]_n$ (1)

The molecular structure of **1** is shown in Figure 1. The iron atom is in an octahedral environment. Besides the two coordinated *trans*-oxygen atoms of the dichromate [Fe1−O1, 2.137(4); Fe1−O4, 2.132(4) Å] with the O1−Fe1−O4 angle of 173.65(13)°, there are four coordinated nitrogen atoms from the 4,4′-bipyridine ligands [Fe1−N1, 2.122(3); Fe1−N2, 2.277(4); Fe1−N3, 2.135(4); Fe1−N4, 2.264(4) Å]. Compared with $[Fe(C_2O_4)(4,4'\text{-bipyridine})]$ and $[FeCl_2(4,4'\text{-bipyridine})]$, the Fe−O and Fe−N bond lengths are in the normal range.[14,15] The non-bridging Cr−O distances are shorter than those of the bridging Cr−O distances. The Cr^{VI} ion adopts an almost regular tetrahedral geometry with an average O−Cr−O bond angle 109.46° for each $[Cr_2O_7]^{2-}$ unit. The Cr−O−Cr bond angle deviates significantly from 180° and is 128.5(2)° in **1**. Surprisingly, there is a 22.4° difference in the two Fe−O−Cr angles [157.9(2)° at O1 vs. 135.5(2)° at O4], although the Fe−O bond lengths are not significantly differ-

[a] Department of Chemistry, Nankai University, Tianjin 300071, P. R. China
Fax: (internat.) + 86-22-23502458,
E-mail: pcheng@nankai.edu.cn

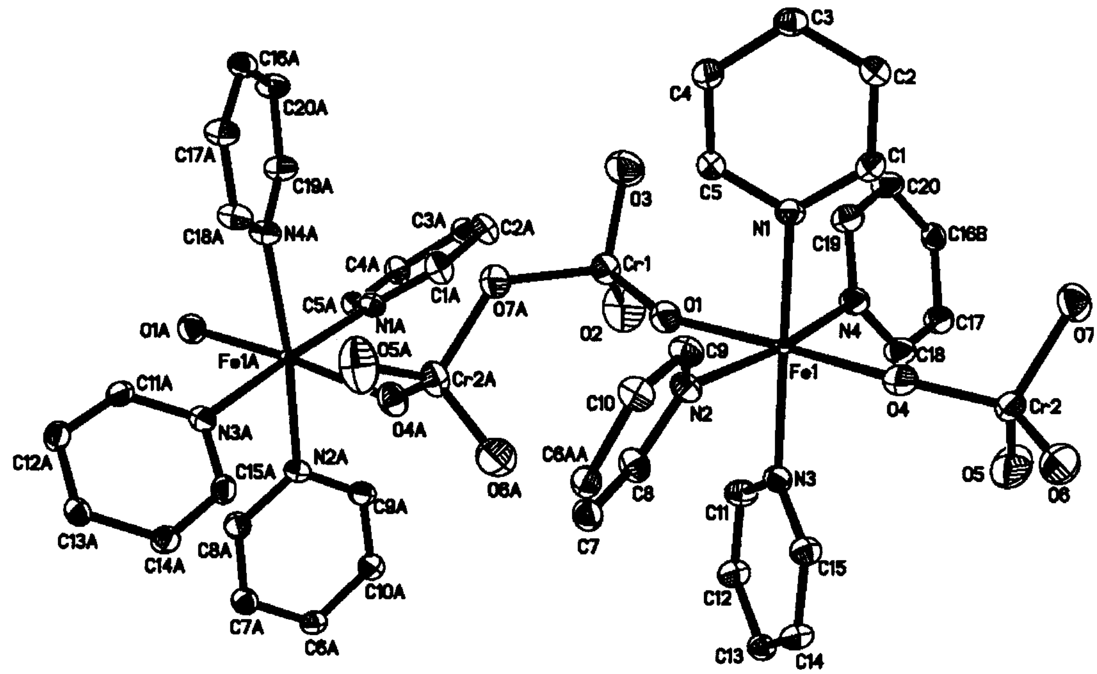

Figure 1. ORTEP diagram of $[Fe(4,4'\text{-bpy})_2Cr_2O_7]_n$ (**1**); the hydrogen atoms and parts of the pyridine rings have been omitted for clarity

ent (Table 1). As a result there are two distinct Fe···Cr distances of 3.702(7) and 3.497(5) Å, which are similar to those of some rare examples of Fe−Cr systems.[10,16]

The structure of **1** contains 2-D parallelogram sheets built upon $[Fe(4,4'\text{-bpy})_2]^{2+}$ building blocks which are cross-linked by dichromate anions like the pillars in clays to form a 3-D structure with two types of channels perpendicular to the (010) and (101) planes, respectively. The rhombic channels with dimensions of 8.859 × 11.472 Å (defined by neighboring Fe···Fe distances) perpendicular to the (010) plane are shown in Figure 2(a), and the square channels with dimensions of 11.436 × 11.472 Å perpendicular to the (101) plane are shown in Figure 2(b).

$[Co(4,4'\text{-bpy})_2Cr_2O_7]_n$ (2)

The structures of **1** and **2** are isostructural except that Fe atoms are replaced by Co atoms. Owing to the difference of the atomic radius, the coordination geometry around the Co^{II} ion is slightly different. The Co^{II} ion is also in an octahedral environment with two *trans*-oxygen atoms of the two dichromate anions in the apical position and four nitrogen atoms of the 4,4′-bpy ligand in the equatorial plane. Similarly, the bridging Cr−O bond lengths [average Cr−O: 1.711(5)Å] are longer than the non-bridging Cr−O bond lengths [average Cr−O: 1.598(5) Å]. The angle O−Co−O is 175.31(14)°. The Cr^{VI} also adopts an almost regular tetrahedral geometry with an average O−Cr−O bond angle of 109.46° for each $[Cr_2O_7]^{2-}$ unit and the Cr−O−Cr bond angle of 128.7(2)° in **2** is similar to that in **1**. There is a 17.6° difference in the two Co−O−Cr angles [157.7(2)° and 140.1(2)°] which is smaller than that observed in compound **1**. Consequently there are also two distinct Co···Cr distances of 3.623(5) and 3.480(4) Å.

In compound **2**, the Co^{II} ions are linked by 4,4′-bpy units in two orthogonal directions and dichromate ions in the third direction thus forming a 3-D structure with two types of channels, similar to **1**. The dimensions of the channels are slightly different: the rhombic channels perpendicular to the (010) plane are 8.790 × 11.436 Å, and the square channels are 11.383 × 11.436 Å perpendicular to the (101) plane.

$[Ni(dpa)_2Cr_2O_7]\cdot H_2O$ (3)

The structure of **3** contains a center of inversion with two $\mu_{1,5}$-dichromate bridges between the two nickel atoms forming a metalla-crown type compound. There has been considerable interest in metalla-crown chemistry owing to its potential applications in chemically modified electrodes, anion-selective separation agents, liquid-crystal precursors and magnetic materials.[17−21]

The Ni···Ni separation of 6.642(5) Å is relatively large, e.g. the Ni···Ni separation in $[Py_2Ni_2(HOOCCMe_3)_2(OOCCMe_3)_2(\mu\text{-}OOCCMe_2)(\mu\text{-}OH_2)]$ is 3.456(2) Å,[22] and two terminal dpa ligands on each nickel complete the ligation (Figure 3). The coordination geometry around the nickel atom is octahedral, the equatorial positions being occupied by three nitrogen atoms from two dpa ligands and one oxygen atom from one bridging dichromate anion [Ni1−O1, 2.071(3) Å]. The axial positions are occupied by the other nitrogen atom of the dpa ligand and one oxygen atom from the other dichromate anion [Ni1−O7A, 2.064(3) Å]. The Ni−N distances ranging from 2.054(4) to 2.075(3) Å are similar to those found in [(oxa)Ni(dpa)] [2.029(2) −2.062(2) Å].[23] Each dpa pyridyl ring is essentially planar and the dihedral angle between the two rings is 35.0°, which is clearly different from other dpa complexes, e.g. in com-

 © 2004 Wiley-VCH Verlag GmbH & Co. KGaA, Weinheim

Table 1. Selected bond lengths [Å] and angles [deg] for **1**, **2**, and **3**

Complex **1**			
Fe(1)−N(1)	2.122(3)	Fe(1)−O(4)	2.132(4)
Fe(1)−O(1)	2.137(4)	Fe(1)−N(3)	2.135(4)
Fe(1)−N(4)	2.264(4)	Fe(1)−N(2)	2.277(4)
Cr(1)−O(2)	1.600(4)	Cr(1)−O(3)	1.610(4)
Cr(1)−O(1)	1.634(4)	Cr(2)−O(6)	1.591(4)
Cr(2)−O(5)	1.603(4)	Cr(2)−O(4)	1.641(4)
Cr(2)−O(7)	1.791(4)		
N(1)−Fe(1)−O(4)	87.16(13)	N(1)−Fe(1)−O(1)	91.78(13)
O(4)−Fe(1)−O(1)	173.65(13)	N(1)−Fe(1)−N(3)	177.50(13)
O(4)−Fe(1)−N(3)	91.03(13)	O(1)−Fe(1)−N(3)	89.83(13)
N(1)−Fe(1)−N(4)	90.19(14)	O(4)−Fe(1)−N(4)	100.04(14)
O(1)−Fe(1)−N(4)	86.22(13)	N(3)−Fe(1)−N(4)	91.82(14)
N(1)−Fe(1)−N(2)	88.74(14)	O(4)−Fe(1)−N(2)	88.72(14)
O(1)−Fe(1)−N(2)	84.99(13)	N(3)−Fe(1)−N(2)	89.49(14)
N(4)−Fe(1)−N(2)	171.11(13)	O(2)−Cr(1)−O(3)	109.7(3)
O(2)−Cr(1)−O(1)	110.4(2)	O(3)−Cr(1)−O(1)	110.1(2)
Complex **2**[a]			
Co(1)−O(7)	2.051(4)	Co(1)−O(3)#1	2.053(3)
Co(1)−N(1)	2.116(4)	Co(1)−N(3)	2.139(4)
Co(1)−N(2)#2	2.207(4)	Co(1)−N(4)#3	2.213(4)
Cr(1)−O(1)	1.591(4)	Cr(1)−O(2)	1.599(4)
Cr(1)−O(3)	1.639(3)	Cr(1)−O(4)	1.780(4)
Cr(2)−O(6)	1.593(4)	Cr(2)−O(5)	1.611(4)
Cr(2)−O(7)	1.648(4)	Cr(2)−O(4)	1.779(4)
O(7)−Co(1)−O(3)#1	175.31(14)	O(7)−Co(1)−N(1)	87.04(14)
O(3)#1−Co(1)−N(1)	91.82(14)	O(7)−Co(1)−N(3)	91.20(14)
O(3)#1−Co(1)−N(3)	89.81(14)	N(1)−Co(1)−N(3)	177.57(15)
O(7)−Co(1)−N(2)#2	88.97(15)	O(3)#1−Co(1)−N(2)#2	86.47(14)
N(1)−Co(1)−N(2)#2	89.26(15)	N(3)−Co(1)−N(2)#2	89.05(14)
N(1)−Co(1)−N(4)#3	90.15(15)	N(3)−Co(1)−N(4)#3	91.74(15)
O(1)−Cr(1)−O(2)	109.2(2)	O(1)−Cr(1)−O(3)	109.7(2)
O(2)−Cr(1)−O(3)	110.3(2)	O(1)−Cr(1)−O(4)	109.8(2)
Cr(2)−O(4)−Cr(1)	128.7(2)	Cr(2)−O(7)−Co(1)	140.1(2)
Complex **3**[b]			
Ni(1)−N(6)	2.054(4)	Ni(1)−N(1)	2.062(3)
Ni(1)−O(7)#1A	2.064(3)	Ni(1)−N(4)	2.070(4)
Ni(1)−O(1)	2.071(3)	Ni(1)−N(3)	2.075(3)
Cr(1)−O(4)	1.597(4)	Cr(1)−O(2)	1.605(3)
Cr(1)−O(1)	1.620(3)	Cr(1)−O(3)	1.761(3)
N(6)−Ni(1)−N(1)	177.87(13)	N(6)−Ni(1)−O(7)#1A	91.85(17)
N(1)−Ni(1)−O(7)#1A	88.24(14)	N(6)−Ni(1)−N(4)	86.65(18)
N(1)−Ni(1)−N(4)	93.39(15)	O(7)#1A−Ni(1)−N(4)	176.10(13)
N(6)−Ni(1)−O(1)	89.39(14)	N(1)−Ni(1)−O(1)	92.74(13)
O(7)#1A−Ni(1)−O(1)	85.93(12)	N(4)−Ni(1)−O(1)	90.45(14)
N(6)−Ni(1)−N(3)	91.60(15)	N(1)−Ni(1)−N(3)	86.28(14)
O(7)#1A−Ni(1)−N(3)	91.36(13)	N(4)−Ni(1)−N(3)	92.28(14)
O(1)−Ni(1)−N(3)	177.15(13)	O(4)−Cr(1)−O(2)	110.1(2)
O(4)−Cr(1)−O(1)	110.28(19)	O(2)−Cr(1)−O(1)	111.31(19)
O(4)−Cr(1)−O(3)	108.20(19)	O(2)−Cr(1)−O(3)	105.76(18)
O(1)−Cr(1)−O(3)	111.02(16)		

[a] #1: $x - 1/2, y + 1/2, z - 1/2$; #2: $x, -y + 1, z - 1/2$; #3: $x, -y, z + 1/2$. [b] #1A: $-x + 2, -y + 1, -z$.

plex $[Cu(dpa)(dca)_2]_n$ the dihedral angle between two pyridine rings of 27.2° is very close to that of free dpa (23°).[24] One nickel atom is coordinated to two dpa units and the large twist serves to relieve the steric hindrance within the ligand.

Despite the fact that the Cr^{VI} adopts an almost regular tetrahedral geometry with an average O−Cr−O bond angle 109.46°, the geometric conformation of the $[Cr_2O_7]^{2-}$ unit in **3** is somewhat different: the Cr−O−Cr bond angle [134.39(19)°] is large compared with those seen in **1** and

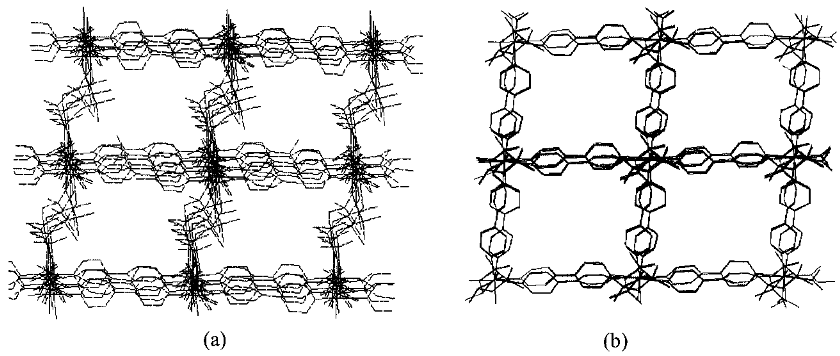

Figure 2. (a) Views of the structure of **1** perpendicular to the (010) plane, showing the rhombic channels; (b) views of the structure of **1** perpendicular to the (101) plane, showing the square channels

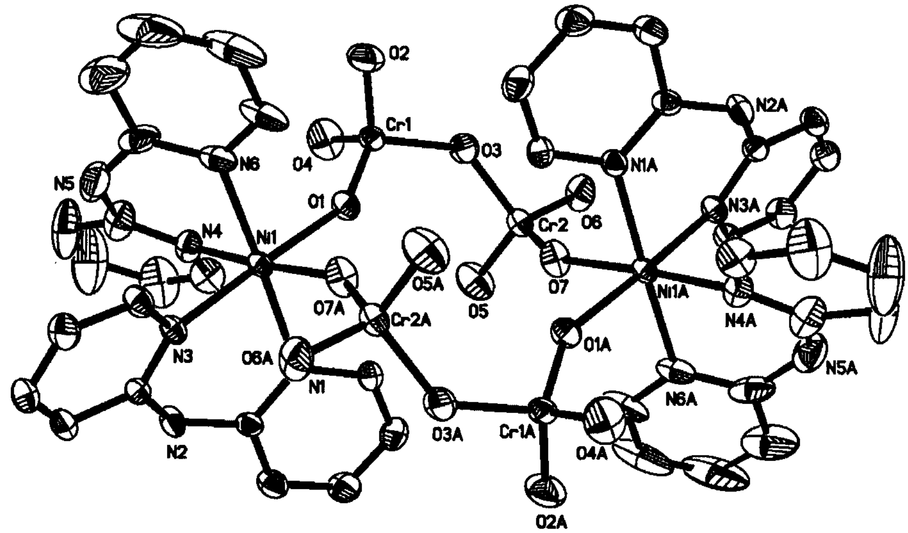

Figure 3. ORTEP diagram of $[Ni(dpa)_2Cr_2O_7]\cdot H_2O$ (**3**), the hydrogen atoms and water molecule have been omitted for clarity

2, and the Ni−O−Cr angles are equal to 151.59(18)°. The widening of the angle at the oxo center may be due to the steric requirements of forming this unusual 12-membered ring. Consequently the Ni···Cr distances are equal to 3.578(5) Å.

The hydrogen atoms of the water molecule in **3** form hydrogen bonds with the nitrogen atoms of neighboring dpa ligands [−H···N, 2.859(3) Å] and uncoordinated oxygen atoms of the bridging dichromate anions [O−H···O, 2.857(8) Å] leading to a 2-D network.

Spectroscopic Properties

The IR spectra of all the complexes show the stretching and bending frequencies of C−C and C−N bonds in the ranges of ca. 1650−1400 cm^{-1} and 1250−650 cm^{-1}, respectively. The ν_{Cr-O} stretching frequencies can be observed at 930−950 cm^{-1} which are in good agreement with those reported for $K_2Cr_2O_7$.[25]

The UV/Vis spectra are also similar. In the UV range, strong absorptions appears at ca. 270−285 nm, which can be assigned to ligand transitions. In the visible region weak absorptions can be observed at ca. 490 nm (spin-forbidden transitions $^5T_{2g}\rightarrow{}^3T_{1g}$, $^3T_{2g}$, ^3E_g) and a relatively stronger absorption at 880 nm ($^5T_{2g}\rightarrow{}^5E_g$) for high-spin Fe^{II} ion can be observed in the spectrum of **1**. A broad strong band centered at ca. 520 nm in the spectrum of **2** can be observed and may be attributed to the d-d transitions of Co^{II} ions in an octahedral environment [$^4T_{1g}\rightarrow{}^4A_{2g}$ and $^4T_{1g}\rightarrow{}^4T_{1g}(P)$]. For complex **3**, the electronic spectrum in the visible range contains a strong absorption band at 630 nm and a weaker one at 475 nm, which are characteristic of an octahedrally coordinated Ni^{II} ion and can be assigned to $^3A_{2g}\rightarrow{}^3T_{1g}$ and $^3A_{2g}\rightarrow{}^3T_{1g}(P)$ transitions, respectively.

Magnetic Properties

The molar magnetic susceptibilities χ_M were measured in the temperature range of 2 to 300 K in a field of 5 KOe for **1**, and 10 KOe for **2** and **3** (Figures 4−7).

As shown in Figure 4, the value of $\chi_M T$ for **1** at 300 K is 2.99 $cm^3\cdot K\cdot mol^{-1}$ (4.89 μ_B) which is close to that of an isolated high-spin Fe^{II} ion ($S = 2$). As the temperature is decreased, the value of $\chi_M T$ decreases gradually and then decreases rapidly in the lower temperature region indicating that a weak antiferromagnetic coupling exists between the

 © 2004 Wiley-VCH Verlag GmbH & Co. KGaA, Weinheim

Fe^{II} ions. In **1**, two exchange pathways are available: one is the inter-chain coupling (via 4,4′-bpy) and the other is the intra-chain interaction (via the dichromate anion). The system was therefore treated using a one-dimensional approach. The Heisenberg exchange theory was utilized, where the Hamiltonian in Equation (1) was employed. The molar magnetic susceptibility per ion is given by the polynomial expression in Equation (2).[26]

$$H = -2J\sum_{i=1}^{N-1} S_i \cdot S_{i+1} \tag{1}$$

$$\chi_{\mathrm{chain}} = (Ng^2\mu_B^2)(kT)^{-1}[(A(s) + [B(s)]\, x^2) \times (1 + [C(s)]x + [D(s)]x^3)^{-1}] \tag{2}$$

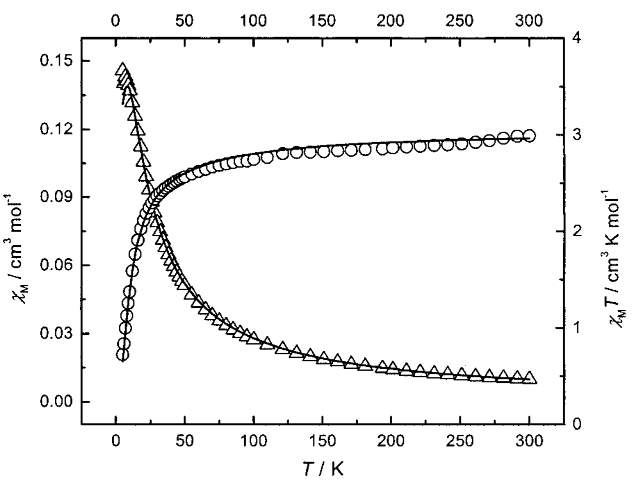

Figure 4. Plots of χ_M (Δ) and $\chi_M T$ (O) versus temperature for **1**; the solid line represents the theoretical curve with the best fit parameters

A molecular field approximation, Equation (3), was then used to modify the inter-chain interaction (zJ') giving the final susceptibility equations of the systems.[27] For the case of the $S = 2$ linear chain, $A = 2.000$, $B = 71.938$, $C = 10.428$, $D = 955.56$, and $x = J / kT$. The best fit of the magnetic susceptibility data yielded $J = -0.74$ cm^{-1}, $zJ' = -0.045$ cm^{-1} and $g = 2.02$. The agreement factor R is 3.65×10^{-4} $\{R = \Sigma[(\chi_M)^{obs} - (\chi_M)^{calc}]^2/[(\chi_M)^{obs}]^2\}$. This result indicates that there are weak antiferromagnetic interactions between the Fe^{II} ions within the chain which may be due to the large Fe···Fe distance and there also exist weak inter-chain antiferromagnetic interactions.

$$\chi_M = \chi_{\mathrm{chain}} / [1 - \chi_{\mathrm{chain}}(2zJ' / Ng^2\beta^2)] \tag{3}$$

For compound **2**, the high-spin octahedral Co^{II} ion has a $^4T_{1g}$ ground state and, as a consequence, exhibits unquenched spin-orbit coupling in addition to zero-field splitting, which dominates in the low-temperature region.[28]

Unfortunately, no expressions account for both factors simultaneously. Therefore, the data for **2** were fit using the expression in Equation (4) (with $x = \lambda/kT$) for spin-orbit coupling. The molecular field approximation which was further considered for the magnetic interactions between cobalt(II) ions and the magnetic susceptibilities is illustrated in Equation (5). The best fit (as shown in Figure 5) was obtained with values of $A = 1.5$, $\lambda = -170.8$ cm^{-1}, $g = 2.19$ and $zJ' = -0.09$ cm^{-1}, where A is a crystal field parameter ($A = 1.5$ is the weak-field limit), λ is the spin-orbit coupling constant ($\lambda = -176.0$ cm^{-1} is the free-ion value). The agreement factor $R = 4.71 \times 10^{-5}$. These are very similar to the published values for the related compound $[Ph_4P][Co\{N(CN)_2\}_3]$ (A = 1.5, λ = −170.0 cm^{-1}).[28] Thus, the fit suggests the presence of cobalt ions with slightly distorted octahedral geometries which is consistent with the crystal structure. The room-temperature magnetic moment of 5.13 μ_B is close to that expected for a weak-field ion (5.20 μ_B), with the slightly lower value indicative of the small perturbation from the ideal octahedral geometry as can be observed in the structure. The value of zJ' indicates a very weak antiferromagnetic exchange interaction between the Co^{II} ions.

$$\chi_M = \frac{N\beta^2}{3kT} \frac{\left[\frac{7(3-A)^2 x}{5} + \frac{12(A+2)^2}{25A} + \left\{\frac{2(11-2A)^2 x}{45} + \frac{176(A+2)^2}{675A}\right\}\exp\left(-\frac{5Ax}{2}\right) + \left\{\frac{(A+5)^2 x}{9} - \frac{20(A+2)^2}{27A}\right\}\exp(-4Ax)\right]}{\frac{x}{3}\left[3 + 2\exp\left(-\frac{5Ax}{2}\right) + \exp(-4Ax)\right]} \tag{4}$$

$$\chi_M = \chi_{Co} / [1 - \chi_{Co}(2zJ' / Ng^2\beta^2)] \tag{5}$$

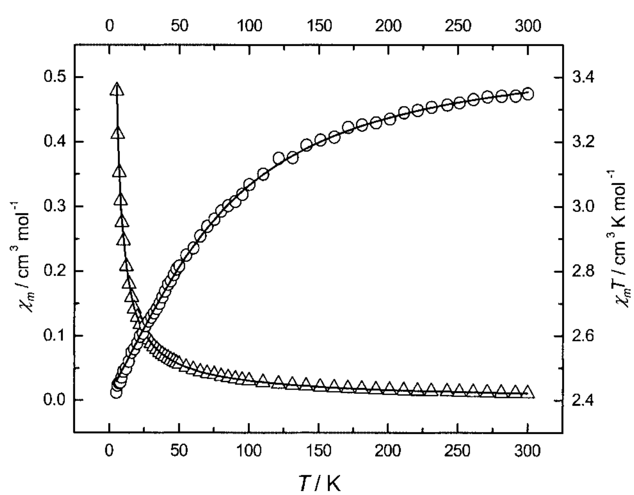

Figure 5. Plots of χ_M (Δ) and $\chi_M T$ (O) versus the temperature for **2**; the solid line represents the theoretical curve with the best fit parameters

The temperature dependence of $\chi_M T$ of **3** is shown in Figure 6. At room temperature $\chi_M T$ is 2.074 cm^3·K·mol^{-1} which is as expected for a spin-only Ni^{II} ion. It continuously increases upon cooling and reaches a maximum value of 2.172 cm^3·K·mol^{-1} at 24 K and further rapidly decreases to 1.85 cm^3·K·mol^{-1} at 2 K. This curve is in agreement with a significant ferromagnetic coupling between the nickel ions whereas in the published literature, most of the dimers with Ni^{II} (d^8) centers have been described as antiferromagnetic.[29−31] Zero-field splitting (D) and inter-

 © 2004 Wiley-VCH Verlag GmbH & Co. KGaA, Weinheim

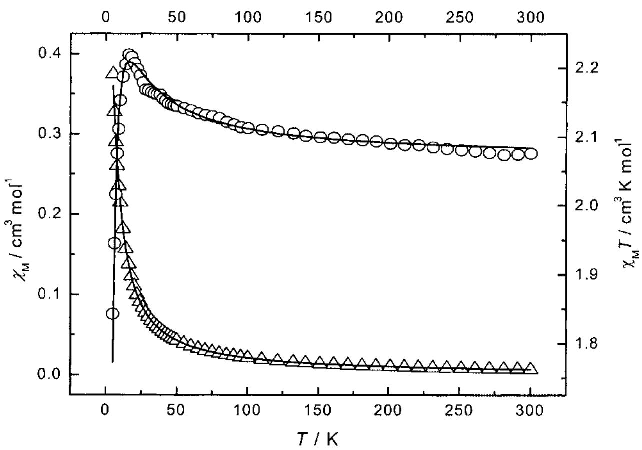

Figure 6. Plots of χ_M (Δ) and $\chi_M T$ (O) versus temperature for **3**; the solid line represents the theoretical curve with the best fit parameters

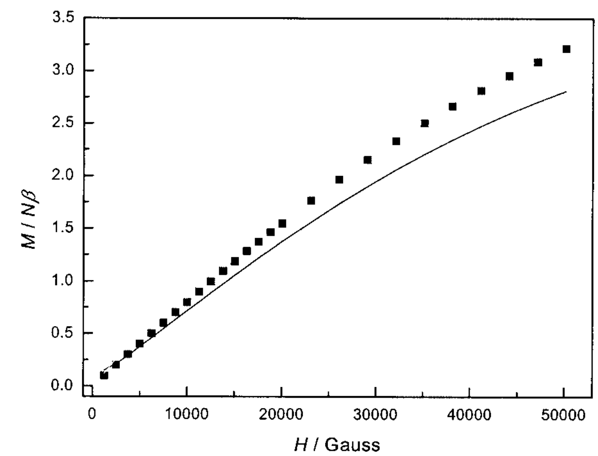

Figure 7. Magnetization curve of **3** (black squares) at 5 K; solid line: Brillouin function corresponding to two uncoupled Ni ions measured at 5 K supports the ferromagnetic interaction in this compound; the experimental values are higher than those calculated by Brillouin functions for two isolated centers with $S = 1$, which confirms the weak ferromagnetic correlation between the two Ni^{II} ions;[35] the effects of single-ion zero-field splitting and inter-dimer interactions cause the rapid low-temperature decrease in $\chi_M T$

molecular interactions could account for the decrease of χ_MT in the lower temperature region.

The nickel dimers contain "octahedrally" coordinated divalent nickel. Since the single-ion ground state is an orbital singlet state, it is appropriate to use the isotropic spin-coupling Hamiltonian [Equation (6)][32] where $\hat{H}_o$ is the Hamiltonian without considering the zero-field splitting and inter-dimer interactions, J is the exchange integral for the intra-dimer interaction between nickel atoms with spin operators $\hat{s}_1$ and $\hat{s}_2$. Since divalent nickel can have a large zero-field splitting parameter, it is necessary to evaluate the effect of single-ion zero-field splitting on the susceptibility. Allowing an external magnetic field H to be applied, the Hamiltonian can be described as shown in Equation (7).[33]

$$\hat{H}_o = -2J\hat{S}_1\cdot\hat{S}_2 \quad (6)$$

$$\hat{H} = -2J\hat{S}_1\cdot\hat{S}_2 - D(\hat{S}_{1z}^2 + \hat{S}_{2z}^2) - g\beta H\hat{S} \quad (7)$$

Taking $g_x = g_z = g$ (a very good approximation for Ni^{2+}), the temperature dependence of the magnetic susceptibilities was calculated using the equation derived from the above Hamiltonian operator.[33,34]

A temperature independent susceptibility term ($N\alpha$) was also include and was set as 2.0×10^{-4} cm^3·mol^{-1}.

A good fit, shown in Figure 6, was obtained for the following parameter set: $g = 2.04$, $J = 1.68$ cm^{-1}, $D = -2.86$ cm^{-1} and $R = 8.96 \times 10^{-5}$. Also the magnetization curve is shown in Figure 7 (0−50 kOe).

According to the above results, the two nickel(II) ions are weakly ferromagnetically coupled through the dichromate anions joining them [Ni···Ni, 6.642(5) Å].

Conclusion

The combined use of the polypyridine system and dichromate anion as ligands towards M^{II} ions [M = Fe (**1**), Co (**2**), Ni (**3**)] allowed us (i) to obtain three new dichromate bridged polymers with the dichromate exhibiting a $\mu_{1,5}$ bridging mode (ii) to study their spectroscopic properties, and (iii) to investigate the efficiency of this mode in mediating exchange interactions between the M^{II} ions. In conclusion, using the dichromate anion to form multi-dimensional systems is quite a useful method for building up multi-dimensional structures. It promises to open a new route for the formation of coordination polymers, which may exhibit interesting topologies and potential properties such as magnetic ordering and spectroscopic or electrical conductivity.

Experimental Section

General Remarks C, H, and N analyses were obtained at the Institute of Elemental Organic Chemistry, Nankai University. IR spectra were recorded in KBr disks on a Shimadzu IR-408 infrared spectrophotometer in the 4000−600 cm^{-1} region. UV/Vis spectra in DMF were recorded on a Shimadzu UV-2101 PC UV/Vis scanning spectrophotometer. Variable-temperature magnetic susceptibilities were measured on a Quantum Design MPMS-7 SQUID magnetometer. Diamagnetic corrections were made with Pascal's constants for all the constituent atoms.

Preparation of [Fe(4,4′-bipy)$_2$Cr$_2$O$_7$]$_n$ (1): An aqueous solution of $(NH_4)_2Fe(SO_4)_2\cdot 6H_2O$ (78.4 mg, 0.2 mmol) and 4,4′-bipyridine (62.5 mg, 0.4 mmol) was heated to reflux for a few minutes. $K_2Cr_2O_7$ (58.8 mg, 0.2 mmol) dissolved in water (5 mL) was then added. The resultant mixture was heated to reflux for 2 h and was then filtered. The filtrate was evaporated at room temperature. Red crystals suitable for X-ray analysis were obtained after a week. Yield: 40%. $C_{20}H_{16}Cr_2FeN_4O_7$: calcd. C 41.12, H 2.76, N 9.59; found C 41.45, H 2.72, N 9.43.

[Co(4,4′-bipy)$_2$Cr$_2$O$_7$]$_n$ (2): The synthetic method here was similar to that used for the preparation of **1** except that

 © 2004 Wiley-VCH Verlag GmbH & Co. KGaA, Weinheim

Table 2. Data collection and processing parameters for **1**, **2**, and **3**.

	1	2	3
Formula	$C_{20}H_{16}Cr_2FeN_4O_7$	$C_{20}H_{16}CoCr_2N_4O_7$	$C_{20}H_{20}Cr_2N_6NiO_8$
Fw	584.22	587.30	635.13
K	273(2)	293(2)	273(2)
Space group	*C*2/*c*	*C*2/*c*	*P*2$_1$/*n*
a (Å)	21.656(9)	21.512(8)	10.158(9)
b (Å)	15.299(6)	15.328(6)	13.855(12)
c (Å)	17.050(7)	16.904(6)	18.475(16)
β (°)	127.130(5)	127.176(6)	102.884(15)
V (Å^3)	4504(3)	4441(3)	2535(4)
Z	8	8	4
ρ (g/cm^3)	1.723	1.757	1.664
μ (mm^{-1})	1.634	1.750	1.633
θ (°)	1.78−25.03	1.78−25.02	1.85−25.02
Index ranges	$-19 \le h \le 25$	$-21 \le h \le 25$	$-12 \le h \le 7$
	$-16 \le k \le 18$	$-17 \le k \le 18$	$-13 \le k \le 16$
	$-20 \le l \le 20$	$-20 \le l \le 9$	$-18 \le l \le 21$
Refl. collected	9026	8891	8835
Independent refl.	3090, R_{int} = 0.0313	3828, R_{int} = 0.0487	4391, R_{int} = 0.0396
Max/min transmission	0.7359 and 0.6400	0.7210 and 0.6218	0.7359 and 0.6400
Data/restraints/parameter	3930/0/307	3828/0/307	4391/0/334
Goodness-of-fit on F^2	1.067	1.020	1.010
R_1, wR_2 [I>2σ(I)]	0.0462, 0.1214	0.0514, 0.1119	0.0409, 0.0903
R_1, wR_2 (all data)	0.0586, 0.1305	0.0767, 0.1205	0.0778, 0.1029
Largest diff. peak and hole (e·Å^{-3})	1.176 and −0.933	0.915 and −0.623	0.644 and −0.312

$(NH_4)_2Fe(SO_4)_2·6H_2O$ was replaced with $Co(ClO_4)_2·6H_2O$. After several days, wine-colored crystals suitable for X-ray analysis were obtained. Yield: 55%. $C_{20}H_{16}CoCr_2N_4O_7$: calc. C 40.90, H 2.75, N 9.54; found C 40.76, H 2.67, N, 9.45.

[Ni(dpa)$_2$Cr$_2$O$_7$]·H$_2$O (3): The synthetic method here was similar to that used for the preparation of **1** except that $(NH_4)_2Fe(SO_4)_2·6H_2O$ and 4,4′-bipyrydine were replaced by $Ni(ClO_4)_2·6H_2O$ and dpa, respectively. Dark green crystals suitable for X-ray analysis were obtained after a week. Yield: 62%. $C_{20}H_{20}Cr_2N_6NiO_8$: calcd. C 37.82, H 3.17, N 13.23; found C 38.04, H 3.35, N 13.14.

Crystallographic Studies: Crystals of **1**, **2**, and **3** having the approximate dimensions of 0.30 mm × 0.25 mm × 0.20 mm were mounted on glass fibers. Determinations of the unit cells and data collection were performed with Mo-*K*α radiation (λ = 0.71073 Å) on a Bruker SMART 1000 diffractometer equipped with a CCD camera. The ω − 2θ scan technique was employed. Crystal parameters and structural refinements for **1**, **2** and **3** are summarized in Table 2. Selected bond lengths and angles are listed in Table 1.

The structures were solved primarily by direct method and secondly by Fourier difference techniques and refined by the full-matrix least-squares method. Computations were performed with the SHELXL-97 program.[36,37] All non-hydrogen atoms were refined anisotropically. The hydrogen atoms were set in calculated positions and refined as riding atoms with a common fixed isotropic thermal parameter.

CCDC-194478 (for **1**), -187395 (for **2**), and -200551 (for **3**) contain the supplementary crystallographic data for this paper. These data can be obtained free of charge via www.ccdc.cam.ac.uk/conts/retrieving.html (or from the Cambridge Crystallographic Data Center, 12 Union Road, Cambridge CB2 1EZ, UK; Fax: + 44-1223-336-033; or E-mail: deposit@ccdc.cam.ac.uk).

Acknowledgments

This work was supported by the National Natural Science Foundation of China (No. 90101028, 50173011) and the Teaching and Research Award Program for Outstanding Young Teachers in Higher Education Institutions of MOE, P. R. C.

[1] O. Kahn, *Molecular Magnetism*; VCH Publishers: New York, **1993**.
[2] S. Kitagawa, M. Kondo, I. Furuchi, M. Munakata, *Angew. Chem. Int. Ed. Engl.* **1994**, *33*, 1759−1761.
[3] M. I. Khan, E. Yohannes, D. Powell, *Inorg. Chem.* **1999**, *38*, 212−213.
[4] S. R. Batten, R. Robson, *Angew. Chem. Int. Ed.* **1998**, *37*, 1461−1494.
[5] O. M. Yaghi, H. Li, T. L. Groy, *Inorg. Chem.* **1997**, *36*, 4292−4293.
[6] H. Oshio, T. Kikuchi, T. Ito, *Inorg. Chem.* **1996**, *35*, 4938−4941.
[7] H. Oshio, H. Okamoto, T. Kikuchi, T. Ito, *Inorg. Chem.* **1997**, *36*, 3201−3203.
[8] H. Oshio, T. Kikuchi, T. Ito, *Chem. Lett.* **2000**, 1138−1139.
[9] P. Chaudhuri, M. Winter, K. Wieghardt, S. Gehring, W. Haase, B. Nuber, J. Weiss, *Inorg. Chem.* **1998**, *37*, 1564−1569.
[10] S. Lorenzo, D. C. Craig, M. L. Scudder, I. G. Dance, *Polyhedron* **1999**, *18*, 3181−3185.
[11] J. T. Park, T. Nishioka, T. Suzuki, K. Isobe, *Bull. Chem. Soc. Jpn.* **1994**, *67*, 1968−1971.
[12] G. De Munno, T. Poerio, M. Julve, F. Lloret, J. Faus, A. Caneschi, *J. Chem. Soc., Dalton Trans.* **1998**, 1679−1685.
[13] A. J. Norquist, K. R. Heier, P. S. Halasyamani, C. L. Stern, K. R. Poeppelmeier, *Inorg. Chem.* **2001**, *40*, 2015−2019.
[14] J. Y. Lu, M. A. Lawandy, J. Li, *Inorg. Chem.* **1999**, *38*, 2695−2704.
[15] M. A. Lawandy, X. Y. Huang, R. J. Wang, J. Li, J. Y. Lu, T. Yuen, C. L. Lin, *Inorg. Chem.* **1999**, *38*, 5410−5414.

[16] B. C. Dave, R. S. Czernuszewicz, *Inorg. Chem.* **1994**, *33*, 847−848.
[17] V. L. Pecoraro, A. J. Stemmler, B. R. Gibney, J. J. Bodwin, H. Wang, J. W. Kampf, A. Barwinski, *Progress in Inorganic Chemistry, Vol. 45* (Ed.: K. D. Karlin), John Wiley & Sons, New York, **1997**, pp. 83−177.
[18] S. X. Liu, S. Lin, B. Z. Lin, C. C. Lin, J. Q. Huang, *Angew. Chem. Int. Ed.* **2001**, *40*, 1084−1086.
[19] J. A. Halfen, J. J. Bodwin, V. L. Pecoraro, *Inorg. Chem.* **1998**, *37*, 5416−5417.
[20] B. Kurzak, E. Farkas, T. Glowiak, H. Kozlowski, *J. Chem. Soc., Dalton Trans.* **1991**, 163−167.
[21] A. J. Stemmler, A. Barwinski, M. J. Baldwin, V. Young, V. L. Pecoraro, *J. Am. Chem. Soc.* **1996**, *118*, 11962−11963.
[22] I. L. Eremenko, S. E. Nefedov, A. A. Sidorov, M. A. Golubnichaya, P. V. Danilov, V. N. Ikorskii, Y. G. Shvedenkov, V. M. Novotortsev, I. I. Moiseev, *Inorg. Chem.* **1999**, *38*, 3764−3773.
[23] J. Y. Lu, T. J. Schroeder, A. M. Babb, M. Olmstead, *Polyhedron* **2001**, *20*, 2445−2449.
[24] J. Carranza, C. Brennan, J. Sletten, F. Lloret, M. Julve, *J. Chem. Soc., Dalton Trans.* **2002**, 3164−3170.
[25] J. B. Bates, L. M. Toth, A. S. Quist, G. E. Boyd, *Spectrochim. Acta, Ser. A* **1973**, *29*, 1585.
[26] W. Hiller, J. Strahle, A. Datz, M. Hanack, W. E. Hatfield, L. W. ter Haar, P. Gutlich, *J. Am. Chem. Soc.* **1984**, *106*, 329−335.
[27] C. J. ÓConnor, *Prog. Inorg. Chem.* **1982**, *29*, 203−206.
[28] J. W. Raebiger, J. L. Manson, R. D. Sommer, U. Geiser, A. L. Rheingold, J. S. Miller, *Inorg. Chem.* **2001**, *40*, 2578−2581.
[29] M. I. Arriortua, A. R. Cortés, L. Lezama, T. Rojo, X. Solans, M. Font Bardía, *Inorg. Chim. Acta* **1990**, *174*, 263−269.
[30] R. Vicente, A. Escuer, J. Ribas, M. Salah el Fallah, X. Solans, M. Font-Bardia, *Inorg. Chem.* **1993**, *32*, 3557−3561.
[31] K. K. Nanda, R. Das, L. K. Thompson, K. Venkatsubramanian, P. Paul, K. Nag, *Inorg. Chem.* **1994**, *33*, 1188−1193.
[32] A. P. Ginsberg, *Inorg. Chim. Acta Rev.* **1971**, *5*, 45.
[33] A. P. Ginsberg, R. L. Martin, R. W. Brookes, R. C. Sherwood, *Inorg. Chem.* **1972**, *11*, 2884.
[34] J. Glerup, P. A. Goodson, D. J. Hodgson, K. Michelson, *Inorg. Chem.* **1995**, *34*, 6255−6264.
[35] Z. E. Serna, L. Lezama, M. K. Urtiaga, M. I. Arriortua, M. G. Barandika, R. Cortés, T. Rojo, *Angew. Chem. Int. Ed.* **2000**, *39*, 344−347.
[36] G. M. Sheldrick, *SHELXS 97, Program for the Solution of Crystal Structures*; University of Göttingen: Germany, **1997**.
[37] G. M. Sheldrick, *SHELXL 97, Program for the Refinement of Crystal Structures*; University of Göttingen: Germany, **1997**.

Received June 27, 2003
Early View Article
Published Online December 19, 2003

 © 2004 Wiley-VCH Verlag GmbH & Co. KGaA, Weinheim